

Simple functional forms for total cross sections from neutron-nucleus collisions

P. K. Deb*

Department of Physics, The Ohio State University, Columbus, OH 43210, USA.

K. Amos†

School of Physics, The University of Melbourne, Victoria 3010, Australia

(Dated: November 3, 2018)

Abstract

Neutron scattering total cross sections have been estimated from nuclei ranging in mass 6 to 238 and for projectile energies 10 MeV to 600 MeV using a simple function of three parameters. These total cross sections have also been calculated using coordinate space optical potentials formed by full folding effective two-nucleon (NN) interactions with one body density matrix elements (OBDME) of the nuclear ground states. Adjusting the theoretical defined parameter values has enabled us to fit the actual measured data. The simple functional parameter values vary smoothly with mass and energy.

PACS numbers: 25.40.-h,24.10.Ht,21.60.Cs

*Electronic address: pdeb@mps.ohio-state.edu

†Electronic address: amos@physics.unimelb.edu.au

I. INTRODUCTION

Neutron-nucleus scattering total cross sections are required in many important fields of study [1]. Scattering complements structure theories and probes the matter distributions. It gives relative motion wave functions which are needed for analyses of other processes; inelastic, charge exchange, particle transfer, capture reactions etc. In Astrophysical studies, reaction cross sections are input to the solar model, supernova evolution (formation and reactions of exotic nuclei) and cosmic model (nucleosynthesis at $t \sim 3$ min). Total cross sections are also needed in disposal of radioactive waste, where using spallation processes, highly radioactive elements are transformed to limit radioactivity to acceptable time periods. In radiation therapy and radiation protection, dosimetry relies on neutron cross sections. Neutron cross sections needed especially for (a) H, C, and O (most abundant in body tissue), (b) Si (shielding material and detectors), (c) N and P (present in tissue and bones), (d) Ca (present in bones), and (e) Al, Fe, Cu, W and Pb (collimation, beam shaping, shielding). In medical radiotherapy absorbed dose distributions in the patient are needed and cannot be measured directly, they must be calculated. For all these purposes an extensive data bank is necessary. Since we do not have the experimental data for all necessary nuclei at all different energies it would be utilitarian if such scattering data were well approximated by a simple convenient function form with which predictions could be made for cases of energies and/or masses as yet to be measured. It has been shown [2, 3, 4, 5] that such forms may exist for proton total reaction cross sections. Herein we consider that concept further to reproduce the measured total cross sections from neutron scattering for energies to 600 MeV and from nine nuclei ranging in mass between ^6Li and ^{238}U . And we show that there is a simple three parameter function form one can use to form estimates without recourse to optical potential calculations. These suffice to show that such forms will also be applicable in dealing with other stable nuclei since their neutron total cross sections vary so similarly with energy [6].

II. FORMALISM

The total and total reaction cross sections for nucleons scattering from nuclei can be expressed in terms of partial wave scattering (S) matrices specified at energies $E \propto k^2$, by

$$S_l^\pm \equiv S_l^\pm(k) = e^{2i\delta_l^\pm(k)} = \eta_l^\pm(k) e^{2i\Re[\delta_l^\pm(k)]}, \quad (1)$$

where $\delta_l^\pm(k)$ are the (complex) scattering phase shifts and $\eta_l^\pm(k)$ are the moduli of the S matrices. The superscript designates $j = l \pm 1/2$. In terms of these quantities, the elastic, reaction (absorption), and total cross sections respectively are given by

$$\sigma_{\text{el}}(E) = \frac{\pi}{k^2} \sum_{l=0}^{\infty} \left\{ (l+1) |S_l^+(k) - 1|^2 + l |S_l^-(k) - 1|^2 \right\} = \frac{\pi}{k^2} \sum_l \sigma_l^{(\text{el})} \quad (2)$$

$$\sigma_{\text{R}}(E) = \frac{\pi}{k^2} \sum_{l=0}^{\infty} \left\{ (l+1) [1 - \eta_l^+(k)^2] + l [1 - \eta_l^-(k)^2] \right\} = \frac{\pi}{k^2} \sum_l \sigma_l^{(\text{R})}, \quad (3)$$

and

$$\begin{aligned} \sigma_{\text{TOT}}(E) &= \sigma_{\text{el}}(E) + \sigma_{\text{R}}(E) = \frac{\pi}{k^2} \left[\sigma_l^{(\text{el})} + \sigma_l^{(\text{R})} \right] = \frac{2\pi}{k^2} \sum_l \sigma_l^{(\text{TOT})}, \\ \sigma_l^{(\text{TOT})} &= (l+1) \{1 - \eta_l^+(k) \cos(2\Re[\delta_l^+(k)])\} + l \{1 - \eta_l^-(k) \cos(2\Re[\delta_l^-(k)])\}. \end{aligned} \quad (4)$$

Therein the $\sigma_l^{(X)}$ are defined as partial cross sections of the total elastic, total reaction, and total scattering itself. For proton scattering, because Coulomb amplitudes diverge at zero degree scattering, only total reaction cross sections are measured. Nonetheless study of such data [3, 5] established that partial total reaction cross sections $\sigma_l^{(R)}(E)$ may be described by the simple function form

$$\sigma_l^{(R)}(E) = (2l + 1) \left[1 + e^{\frac{(l-l_0)}{a}} \right]^{-1} + \epsilon (2l_0 + 1) e^{\frac{(l-l_0)}{a}} \left[1 + e^{\frac{(l-l_0)}{a}} \right]^{-2}, \quad (5)$$

with the tabulated values of $l_0(E, A)$, $a(E, A)$, and $\epsilon(E, A)$ all varying smoothly with energy and mass. Those studies were initiated with the partial reaction cross sections determined by using complex, non-local, energy-dependent, optical potentials generated from a g -folding formalism [7]. While those g -folding calculations did not always give excellent reproduction of the measured data (from ~ 20 to 300 MeV for which one may assume that the method of analysis is credible), they did show a pattern for the partial reaction cross sections that suggest the simple function form given in Eq. (5). With that form excellent reproduction of the proton total reaction cross sections for many targets and over a wide range of energies were found with parameter values that varied smoothly with energy and mass.

Herein we establish that total cross sections for scattering of neutrons from nuclei can also be so expressed and we suggest forms, at least first average result forms, for the characteristic energy and mass variations of the three parameters involved. Nine nuclei, ^6Li , ^{12}C , ^{19}F , ^{40}Ca , ^{89}Y , ^{184}W , ^{197}Au , ^{208}Pb and ^{238}U , for which a large set of experimental data exist, are considered.

III. RESULTS AND DISCUSSIONS

While we have used the partial total cross sections from microscopic results for neutron scattering from all the nine nuclei chosen and at all of the energies indicated, only those obtained for ^{208}Pb are shown in Fig. 1. The results from calculations of scattering from the other eight nuclei have similar form. The ‘data’ shown as blue dashed lines in Fig. 1 are the values found from the g -folding optical model calculations. Each black curve shown therein is the result of a search for the best fit values of the three parameters, l_0 , a , and ϵ that map Eq. (5) (now for total neutron cross sections) to these ‘data’.

From the sets of values that result from the fitting process, the two parameters a and ϵ can themselves be expressed by the parabolic functions

$$\begin{aligned} a &= 1.29 + 0.00250 E - 1.76 \times 10^{-6} E^2, \\ \epsilon &= -1.47 - 0.00234 E + 4.16 \times 10^{-6} E^2, \end{aligned} \quad (6)$$

where the target energy E is in MeV. There was no conclusive evidence for a mass variation of them. With a and ϵ so fixed, we then adjusted the values of l_0 in each case so that actual measured neutron total cross-section data were fit using Eq. (5). Numerical values for l_0 from that process are presented in a table in Ref. [8]. The values of l_0 increase monotonically with both mass and energy and that is most evident in Fig. 2, where the optimal values $l_0(E)$ are presented as different patterned and colored lines. The set for each of the masses (from 6 to 238) are given by those that increase in value respectively at 600 MeV. While that is obvious for most cases, note that there is some degree of overlap in the values for ^{197}Au and for ^{208}Pb .

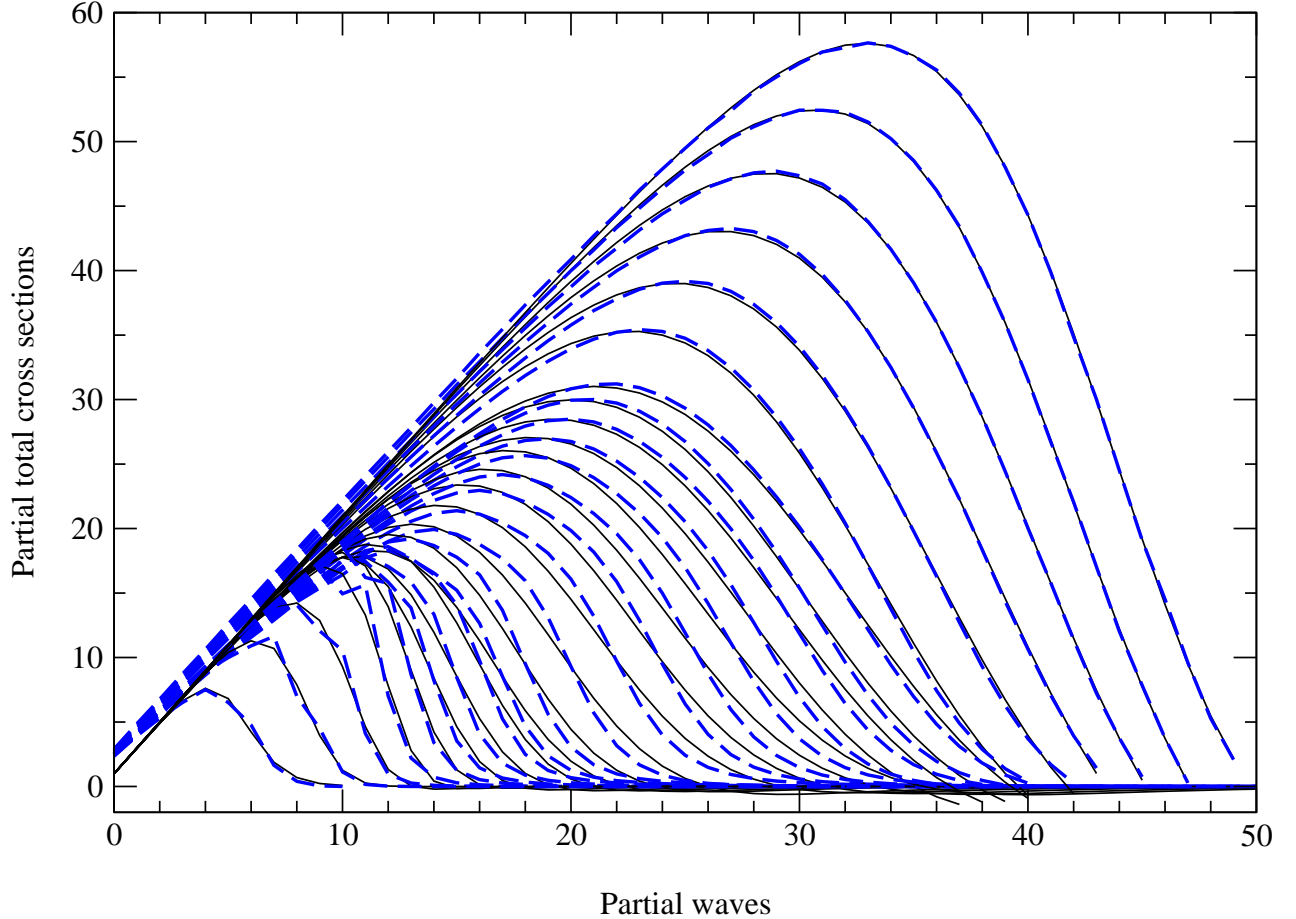


FIG. 1: The partial total cross sections for scattering of neutrons from ^{208}Pb with the set of energies between 10 and 600 MeV specified in the text. The largest energy has the broadest spread of values.

The total neutron scattering cross sections generated using the function form for partial total cross sections with the tabled values of l_0 and the energy function forms of Eq. (6) for a and ϵ , are shown in Figs. 3, 4, 5, 6, and 7. They are displayed by the solid red lines that closely match the data which are portrayed by blue open circles. The data that was taken from a survey by Abfalterer *et al.* [9] which includes data measured at LANSCE that are supplementary and additional to those published earlier by Finlay *et al.* [10]. For comparison we show results obtained from calculations made using g -folding optical potentials [11]. Dashed green lines represent the predictions obtained from those microscopic optical potential calculations. Clearly for energies 300 MeV and higher, those predictions fail.

Predictions of the total cross sections for neutrons scattered from ^6Li and ^{12}C are compared to the data in Fig. 3 and those from ^{19}F and ^{40}Ca are compared to the data in Fig. 4.

Dashed green lines represent the results obtained from full folding optical potential calculations and the solid red lines show the results obtained from functional form calculations. In Fig. 3, g folding results for ^6Li reflect the observed data well from 30 MeV to 600 MeV, but overpredicted for the energies lower than 30 MeV. For ^{12}C , g folding results reproduce the data very well for the energy range from 30 MeV to 200 MeV, but underpredicted for

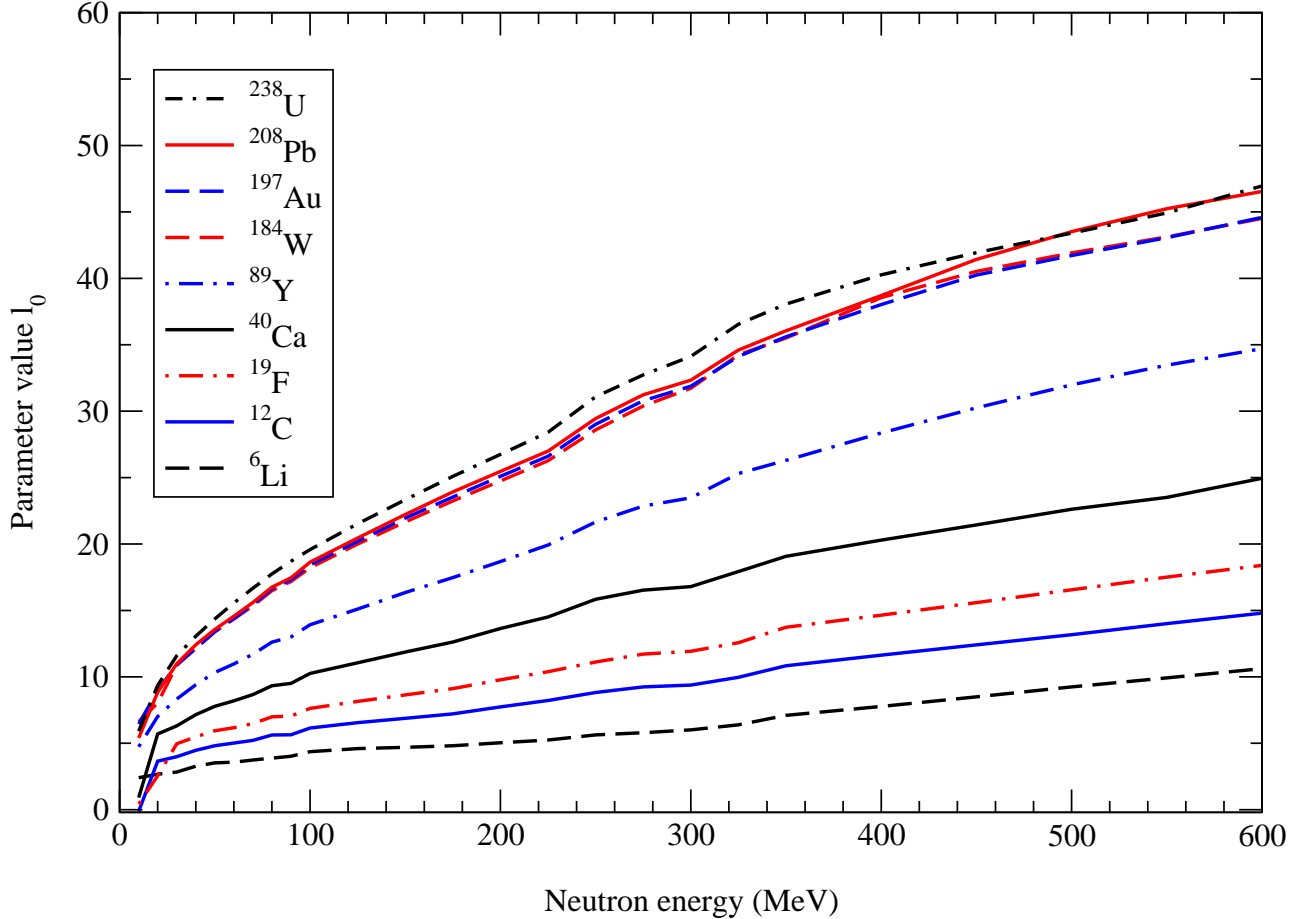


FIG. 2: The values of l_0 that fit neutron total scattering cross-section data from the nine nuclei considered and for energies between 10 and 600 MeV. The curves portray the best fits found by taking a function form for $l_0(E)$.

the energies lower than 30 MeV and higher than 200 MeV. For ^{19}F and ^{40}Ca cases, in Fig. 4, data fits well with the g -folding results for the energy range 100 MeV–200 MeV, but underpredicted for less than 100 MeV and greater than 200 MeV. The peaks at 30 MeV for ^{19}F and at 40 MeV for ^{40}Ca are underpredicted by the g -folding results. Excellent reproductions of data made by functional form results for all cases.

Our predictions for the total cross sections for neutrons scattering from ^{89}Y , and ^{184}W are compared to the data in Fig. 5 and those for ^{197}Au , and ^{238}U are compared to the data in Fig. 6. In Fig. 5, for ^{89}Y , results predicted from g -folding calculations agree with the experimental data for the energy range between 10 MeV to 30 MeV and 90 MeV to 200 MeV, otherwise underpredicted. For ^{184}W , g -folding results agree with the data for the energy range between 70 MeV to 250 MeV, but overpredict the data for the energy range between 10 MeV to 70 MeV and underpredict for the energy above 250 MeV. In Fig. 6, for ^{197}Au and ^{238}U cases, g -folding results reflects the data well for the energies below 200 MeV but overpredicted for the energies above 200 MeV. In both cases, the peaks near 40 MeV are overpredicted and peaks near 80 MeV are underpredicted by the results obtained from g -folding calculations. Functional form results are in excellent agreement with the data in all cases.

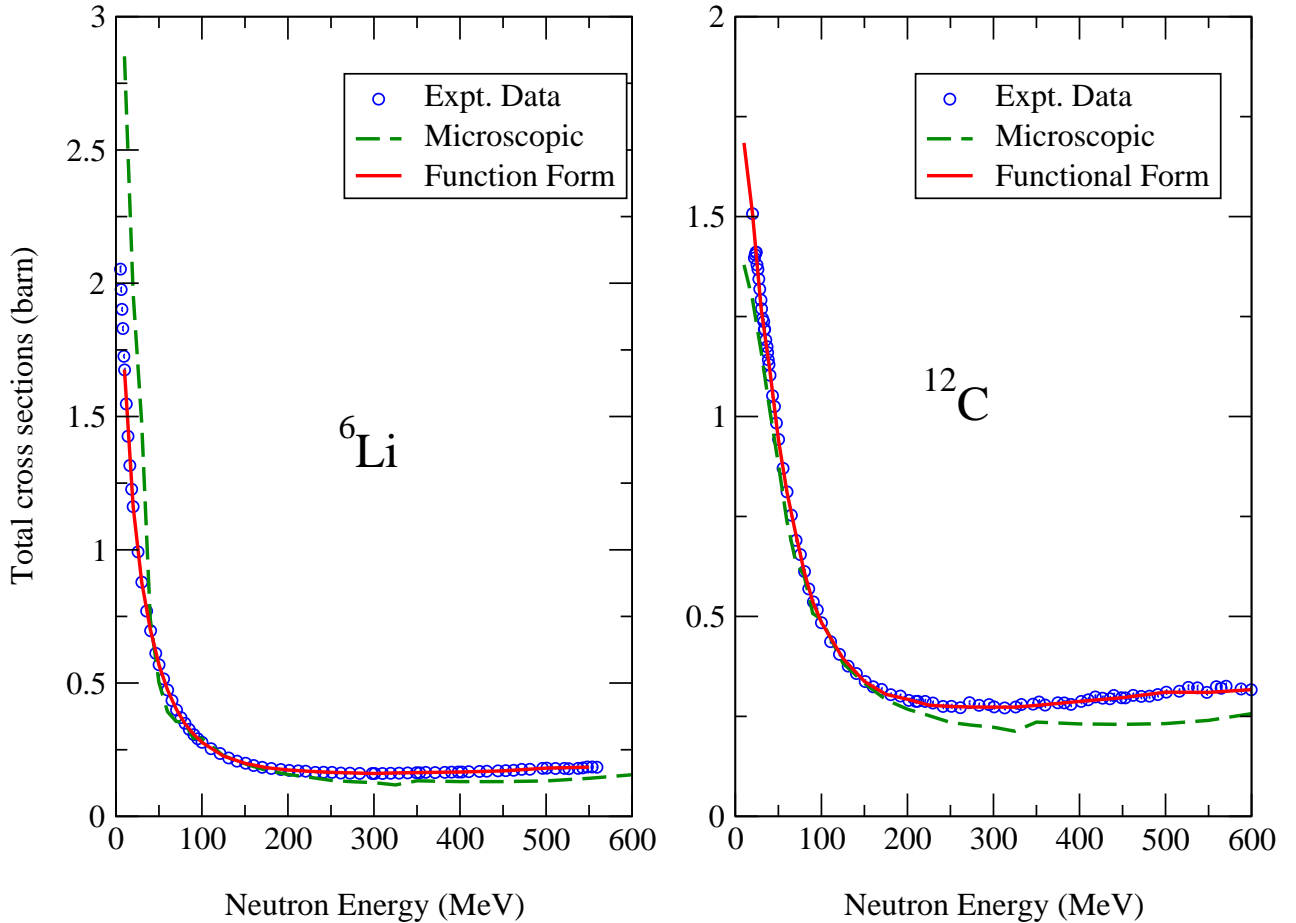


FIG. 3: Total cross sections for neutrons scattered from ${}^6\text{Li}$ (left) and ${}^{12}\text{C}$ (right).

We show in Fig. 7, the results for neutron scattering from ${}^{208}\text{Pb}$. In this case we used Skyrme-Hartree-Fock model (SKM*) densities [12] to form the g -folding optical potentials. That structure when used to analyze proton and neutron scattering differential cross sections at 65 and 200 MeV gave quite excellent results [13]. Indeed those analyzes were able to show selectivity for that SKM* model of structure and for the neutron skin thickness of 0.17 fm that it proposed.

Using the SKM* model structure, the g -folding optical potentials gave the total cross sections shown by the dashed green curve in Fig. 7. Of all the results, we believe these for ${}^{208}\text{Pb}$ point most strongly to a need to improve on the g -folding prescription as is used currently when energies are at and above pion threshold. Nonetheless, it does do quite well for lower energies, most notably giving a reasonable account of the Ramsauer resonances [6] below 100 MeV. However, as with the other results, these g -folding values serve only to define a set of partial cross sections from which an initial guess at the parameter values of the function form is specified. With adjustment that form produces the solid red curve shown in Fig. 7, which is an excellent reproduction of the data, as it was designed to do. But the key feature is that the optimal fit parameter values still vary smoothly with mass and energy.

Without seeking further functional properties of the parameters, one could proceed as we have done this far but by using many more cases of target mass and scattering energies so

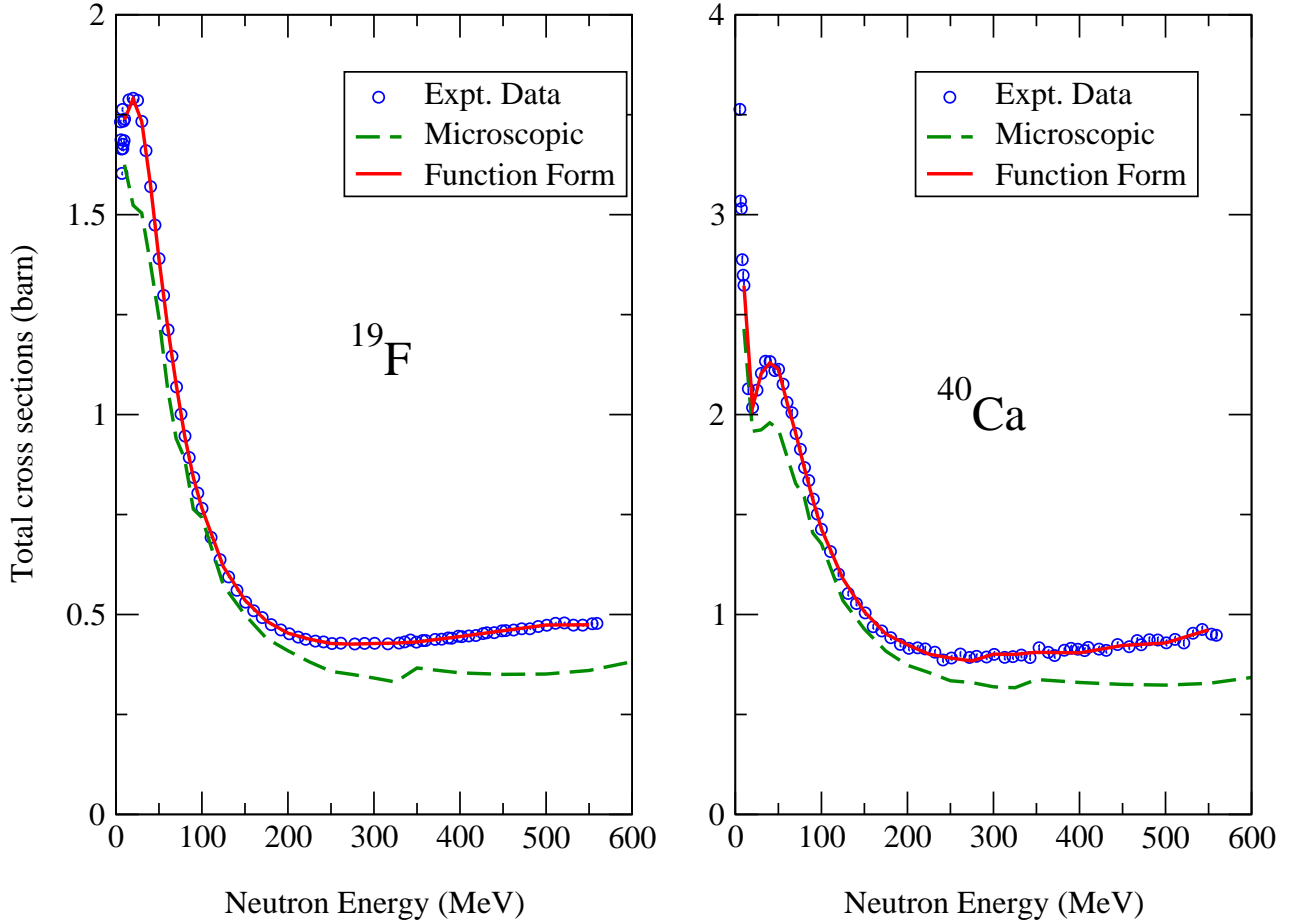


FIG. 4: Total cross sections for neutrons scattered from ^{19}F (left) and ^{40}Ca (right).

that a parameter tabulation as a data base may be formed with which any required value of total scattering cross section might be reasonably predicted (i.e. to within a few percent) by suitable interpolation on the data base, and the result used in Eq. (5).

IV. CONCLUSIONS

Total cross sections for 10 to 600 MeV neutron scattering from nuclei ranging in mass from ^6Li to ^{238}U calculated by simple functional form are in excellent fit to the experimental data. We suggest the three parameter function form for partial total cross sections that will give neutron total cross sections without recourse to phenomenological optical potential parameter searches. That functional form also reproduces proton reaction cross sections. The parameters that fit actual data show smooth trends with both energy and target mass.

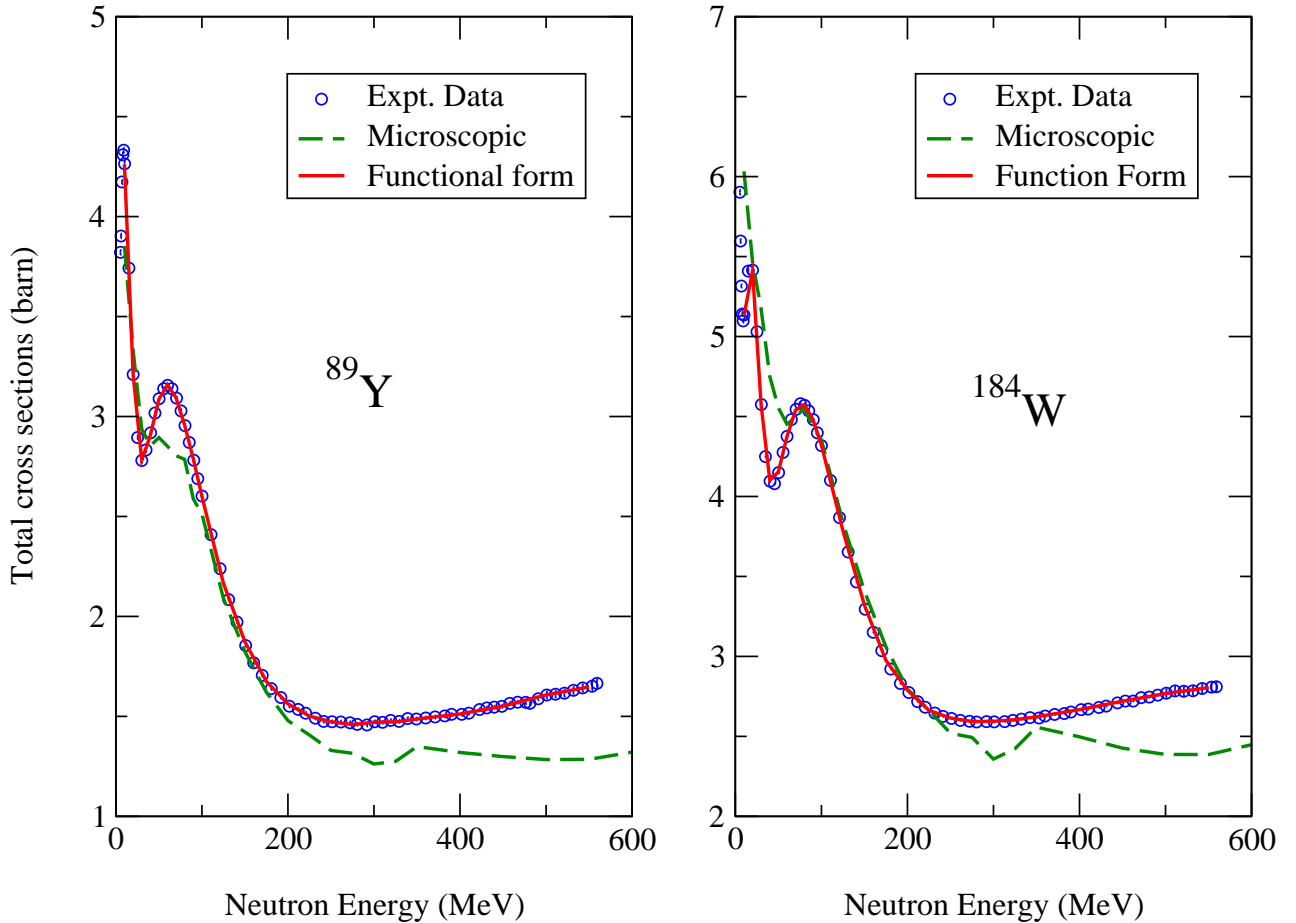


FIG. 5: Total cross sections for neutrons scattered from ^{89}Y (left) and ^{184}W (right).

Acknowledgments

This research was supported by a research grant from the Australian Research Council and also by the National Science Foundation under Grant No. 0098645.

[1] P. K. Deb and K. Amos, arXiv:nucl-th/0407027 (2004).
 [2] S. Majumdar, P. K. Deb, and K. Amos, Phys. Rev. C **64**, 027603 (2001).
 [3] K. Amos and P. K. Deb, Phys. Rev. C **66**, 024604 (2002).
 [4] K. Amos, P. K. Deb, S. Karatagliidis, and D. G. Madland, J. Nucl. Sci. Technol. **2**, 738 (2002).
 [5] P. K. Deb and K. Amos, Phys. Rev. C **67**, 067602 (2003).
 [6] A. J. Koning and J. P. Delaroche, Nucl. Phys. A **713**, 231 (2003).
 [7] K. Amos, P. J. Dortmans, H. V. von Geramb, S. Karatagliidis, and J. Raynal, Adv. in Nucl. Phys. **25**, 275 (2000).
 [8] P. K. Deb and K. Amos, Phys. Rev. C **69**, 064608 (2004).
 [9] W. P. Abfalterer, F. B. Bateman, F. S. Dietrich, R. W. Finlay, R. C. Haight, and G. L. Morgan, Phys. Rev. C **63**, 044608 (2001).

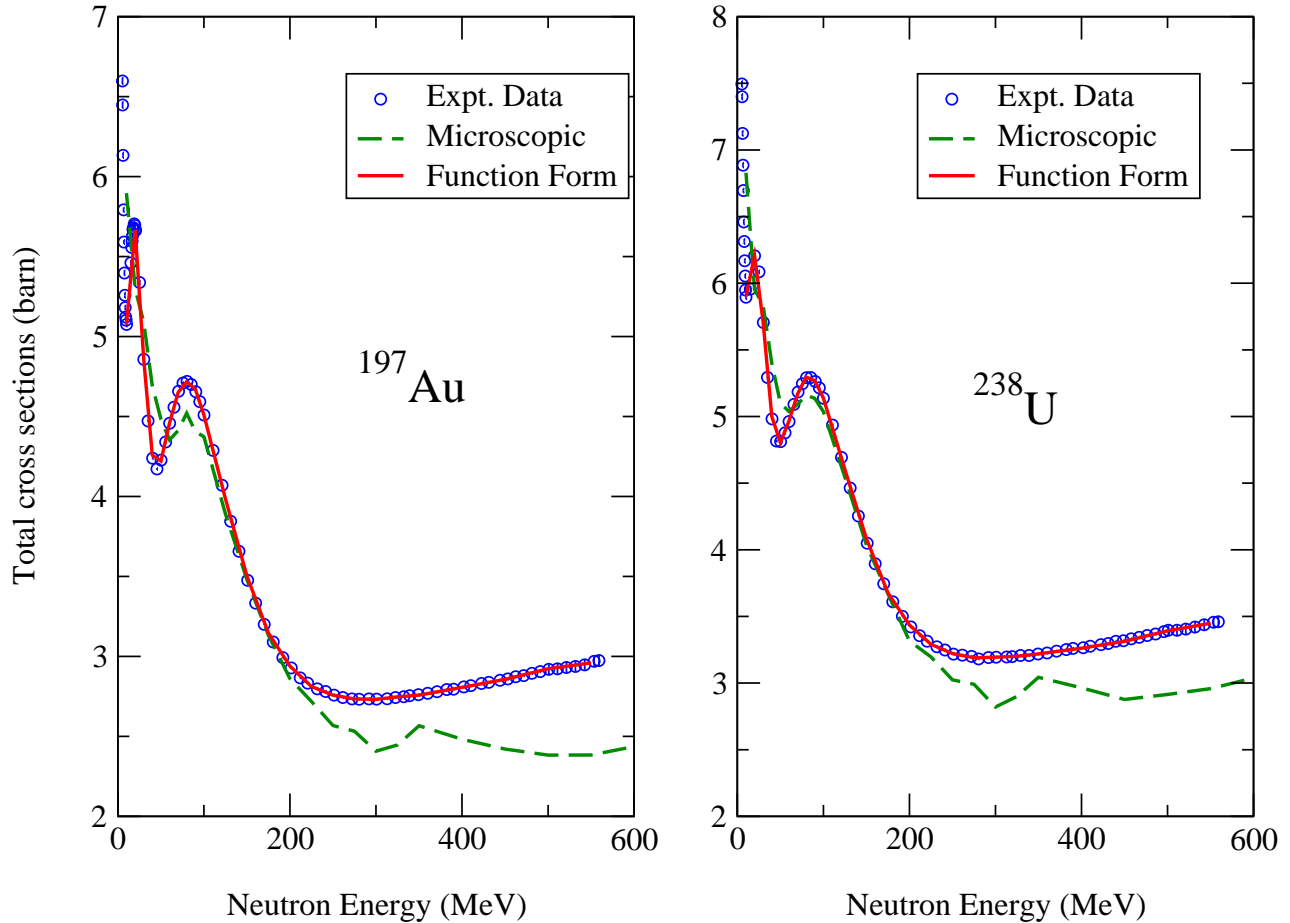


FIG. 6: Total cross sections for neutrons scattered from ^{197}Au (left) and ^{238}U (right).

- [10] R. W. Finlay, W. P. Abfalterer, G. Fink, E. Monte, T. Adami, P. W. Lisowski, G. L. Morgan, and R. C. Haight, Phys. Rev. C **47**, 237 (1993).
- [11] K. Amos, S. Karataglidis, and P. K. Deb, Phys. Rev. C **65**, 064618 (2002).
- [12] B. A. Brown, Phys. Rev. Lett. **85**, 5296 (2000).
- [13] S. Karataglidis, K. Amos, B. A. Brown, and P. K. Deb, Phys. Rev. C **65**, 044306 (2002).

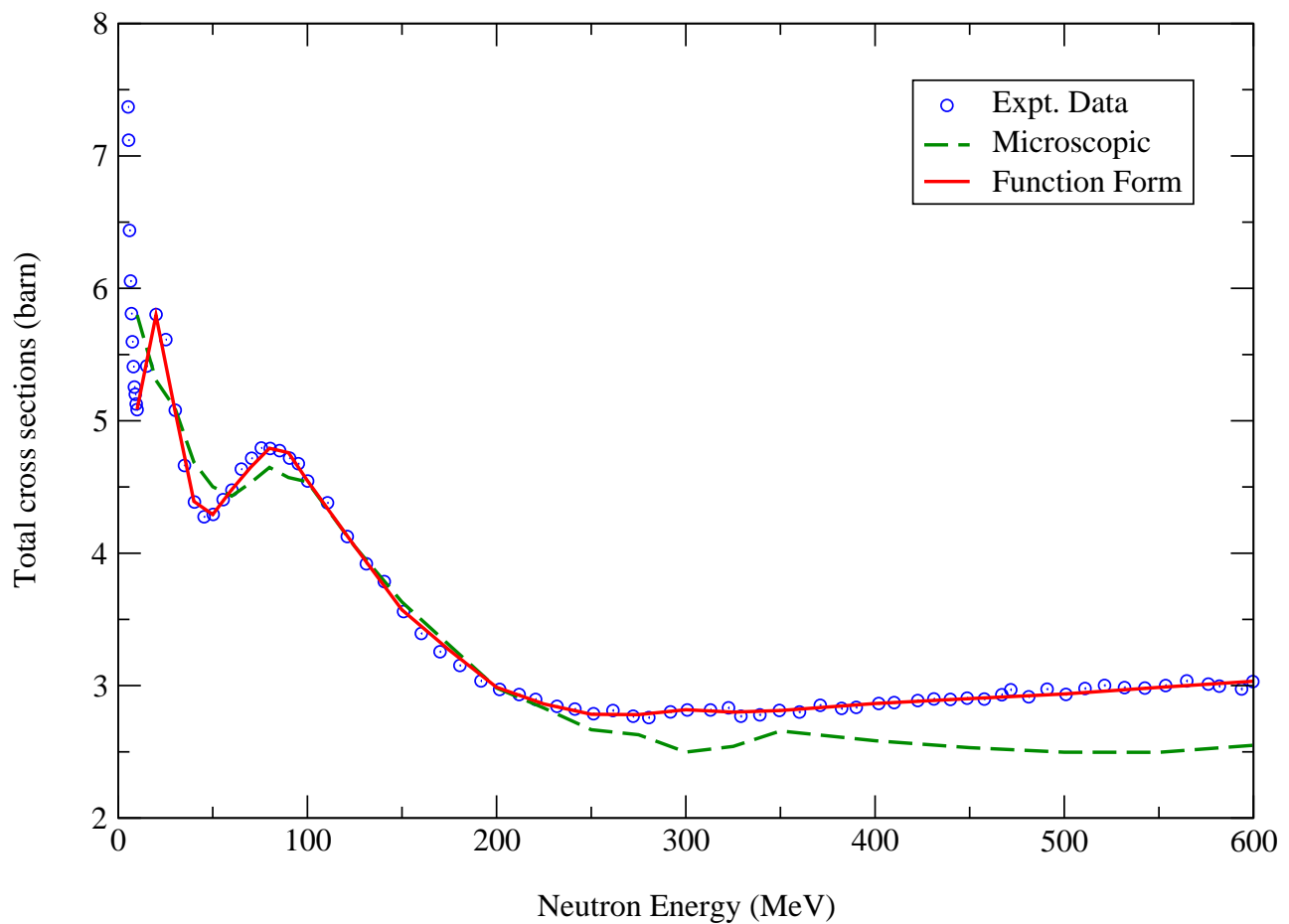


FIG. 7: Total cross sections for neutrons scattered from ^{208}Pb .